Characterizing the Full Range of Stellar Populations in the Outskirts of Galaxies

Principal Investigator: Daniel A. Dale

Institution: University of Wyoming

Electronic mail: ddale@uwyo.edu

Technical Contact: Daniel A. Dale, University of Wyoming

Co−Investigators: Kate Barnes, Indiana University

Daniela Calzetti, University of Massachusetts

Armando Gil de Paz, Universidad Complutense de Madrid

Shawn Staudaher, University of Wyoming

David Thilker, Johns Hopkins University

Liese van Zee, Indiana University

Science Category: Extragalactic: nearby galaxies (z<0.05, v_sys<15,000 km/s)

Observing Modes: IRAC Post−Cryo Mapping

Hours Requested: 133.9

Proprietary Period(days): 365

Abstract:
The understanding of galaxy evolution hinges on unraveling the detailed star formation history and obtaining a full census of the stellar populations of galaxies across all environments, from the inner disks to the extreme outer regions. We propose to observe the mid−infrared emission of the outer disks of a carefully selected sample of nearby galaxies for which extensive ancillary data are available, including deep ultraviolet, broadband optical, and H−alpha narrow band imaging. Our observations aim at fully characterizing the nature of the recently−discovered extended ultraviolet disks, by probing the evolved stellar populations in those extreme locales. The ultraviolet−to−mid−infrared spectral energy distributions of the outer regions will provide their star formation histories and stellar masses, which we will compare with extant models of galaxy formation, including inside−out and accretion. This project provides a systematic approach to the investigation of outer disk regions, and greatly extends over previous similar programs, which have provided only a piecemeal view of such regions. Our warm mission survey will represent a landmark reference for complementary investigations of local galaxies and a benchmark for studies of distant galaxies in the era of JWST.

1   Science Plan

1.1   Scientific Justification

1.1.1   Old Stars in Extended Ultraviolet Disks

The size of a galaxy is a fundamental parameter in our understanding of the evolution of galaxies. In λCDM models, galactic disks are built through mergers and the accretion of small satellites, as well as through *in situ* star formation activity (e.g., Abadi et al. 2003; Governato et al. 2004). These two growth mechanisms have distinctly different predictions for the age of the associated extended stellar population.

According to the inside-out galaxy formation scenario, the outer disk should be dominated by a smoothly distributed young population of stars (Avila-Reese & Firmani 2000). In this model, outer disk stars were either formed from star formation occurring in the galaxy outskirts, or they were transported from the inner disk regions through 'radial migration' (Roškar et al. 2008). GALEX observations carried out in the ultraviolet have shown the young stellar distribution to extend well beyond $2R_{25}$ in the so-called extended ultraviolet disk or 'XUV' galaxies (Thilker et al. 2007; Gil de Paz et al. 2007; Zaritsky & Christlein 2007). These galaxies in turn typically have disks with rich HI outer envelopes.

In contrast to inside-out disk formation scenarios, accretion models predict that the diffuse, outermost stellar distribution is largely composed of the remnants of previously accreted satellites and tidal debris from major mergers, and thus is dominated by an older stellar population that likely exhibits substructure (Robertson et al. 2004). The Keck-based work of Ibata et al. (2005) presents such a scenario for M 31: they find stars associated with that galaxy as far as 70 kpc ($1.6R_{25}$) from the nucleus, and with velocities close to those expected for circular orbits at that distance. This stellar emission shows substructure, consistent with an accretion history.

Similarly, Thilker et al. (2005) find knots of ultraviolet emission extending out to $4R_{25}$ in M 83, a galaxy known to have substructure in its outer disk, perhaps due to a recent (1–2 Gyr ago) encounter with NGC 5253 (Rogstad et al. 1974; van den Bergh 1980). Dong et al. (2008) use GALEX and IRAC to determine the ages and stellar masses of stars in the extended ultraviolet disk of M 83, finding typical ages of 100–200 Myr, but extending up to over a Gyr. Similar results are obtained by Alberts et al. (2010) for a sample of five XUV galaxies. Likewise, Gogarten et al. (2009) find long durations for the star formation history of the outer disk of M 81. Finally, in another study of extended stellar emission in local galaxies, Herbert-Fort et al. (2009) use deep LBT and GALEX imaging to probe the blue and red stellar populations in NGC 3184. In this galaxy red stellar clusters are more prominent than their blue counterparts at the largest radii, and in fact, the red knots appear to be correlated with the outermost fringes of the HI emission at $1.7R_{25}$.

The local extended ultraviolet disk fraction has been estimated to be $\sim30\%$ (Thilker et al. 2007; see also Zaritsky & Christlein 2007). Thilker et al. (2007) separate the XUV galaxies into two classes. Type 1 disks frequently contain filamentary, outer disk substructure, perhaps indicative of an accretion history or interaction-driven evolution, whereas Type 2 XUV galaxies exhibit an ultraviolet profile smoothly extending from the interior to the outer disk regions. Interestingly, Thilker et al. find a 2-to-1 ratio of Type 1 to Type 2 XUV disks. Also interesting is that approximately 30% of optical surface brightness profiles from SDSS data on nearby galaxies show "anti-truncation" (upbending) in the outer regions (e.g., Pohlen & Trujillo 2006).

All of these results demonstrate a complex variety of morphology at different wavelengths in the outer disk environment. Does the Type 1 to Type 2 ratio reflect the ratio of accretion-to-inside-out formation scenarios? Do the studies on individual galaxies described above suggest that extended *optical* disks are commonplace locally? Are XUV galaxies typically also 'XOpt' galaxies? An extremely deep near-infrared survey of the evolved stellar population and its mass surface density, color, and substructure would yield crucial insights to the fossil record in galaxy peripheries, and make great strides toward answering these questions.

1.1.2   Old Stars and Hα emission in Galaxy Peripheries

Star formation has long been thought to occur only above a certain threshold in gas density (e.g., Schmidt 1959; Kennicutt 1998; Leroy et al. 2008; Krumholz, McKee, & Tumlinson 2009; Bush et al. 2010). Like most other tracers of the interstellar medium, the neutral and molecular gas surface brightness profiles decrease at large radii (e.g., Regan et al. 2006), and thus it is not surprising that Hα surface brightness profiles typically show a sharp truncation near the R_{25} optical edge of galaxies (e.g., Martin & Kennicutt 2001). However, spurred in part by the discovery of XUV disks, recent Hα observations in the outer disks of galaxies have shown a more complicated situation, with some Hα profiles extending to 1.5–$2R_{25}$ (Christlein, Zaritsky, & Bland-Hawthorn 2010; Goddard, Kennicutt, & Ryan-Weber 2010).

An intriguing related result stems from a comprehensive UV+IR+Hα survey of ∼300 galaxies within the Local Volume out to 11 Mpc (Kennicutt et al. 2008). At very low star formation activity levels, down to star formation rates of $\sim 10^{-4}$ $M_\odot$ yr^{-1} that are comparable to the environments in the outer disks of normal galaxies, Lee et al. (2009) find that Hα systematically underestimates the star formation rate relative to the far-ultraviolet (see also Meurer et al. 2009). This finding is not a result of extinction, since the far-ultraviolet continuum is more impacted than Hα by dust attenuation. Moreover, the discrepancy in these star formation rate indicators are shown by Lee et al. to unlikely be due to stellar evolutionary model uncertainties, metallicity, bursty star formation histories, ionizing photon leakage, or stochasticity in the formation of high-mass stars. The most compelling alternative is a steeper initial mass function for regions of low star formation activity such as in dwarf low surface brightness galaxies, resulting in a deficit of high-mass stars for dwarf galaxies, a scenario supported by theoretical predictions (Kroupa & Weidner 2003; Weidner & Kroupa 2005, 2006; Pflamm-Altenburg et al. 2007, 2009). However, in contrast to this picture, comparisons of far-ultraviolet, near-ultraviolet, and Hα data in the outer disks of nearby galaxies point to stochasticity in high-mass star formation as the culprit for differences between Hα- and UV-based star formation rates in outer disks, and provide no evidence for an IMF that is unique to such peripheral environments (e.g., Goddard, Kennicutt, & Ryan-Weber 2010; Alberts et al. 2010). Clearly a more detailed set of multi-wavelength data is needed to better understand the origin and nature of star formation in the outskirts of galaxies. For example, it would be important to determine if the stellar masses obtained from our deep IRAC imaging of the outer disks are consistent with those inferred from the star formation histories computed from the collection of ultraviolet, optical, and infrared data.

1.1.3   Summary of Science Goals

We propose to obtain very deep 3.6 μm imaging of a sample of nearby galaxies, with a primary goal of quantifying how far out the old stellar population can be detected. Do they extend as far out as the star formation measured on ∼5 Myr timescales as traced by Hα? Do

they extend as far out as the star formation measured on ~100 Myr timescales as traced by the ultraviolet? Do they show similar radial truncation properties as observed in Hα and the ultraviolet? Is there a characteristic mass surface density for XUV disks, which could provide a unique method for detecting UV-dormant extended galaxies? Another science goal is to utilize IRAC and GALEX data to determine the ages of the outer disk stellar populations. Determining the stellar ages in the outer disks will help to differentiate between an inside-out galaxy formation scenario and an accretion-based one, where theoretical predictions suggest younger stars for the former scenario and older stars for the latter. Likewise, if a young stellar population in the outer disk appears clumpy or smooth, does the old stellar population have a similar morphology? Such information could help confirm or reject formation by accretion. Finally, we plan to utilize the proposed deep IRAC imaging and the ancillary ultraviolet and optical data to determine whether the stellar masses in the extended disks are consistent with those inferred from their star formation histories.

1.1.4 Why *Spitzer*?

The apparent size of a galaxy depends on the emission mechanism in question (stellar light, synchrotron radiation, thermal emission from dust, etc.), along with the sensitivity of the measurement. One of our goals is to simply compare the full extent of the stellar disk traced by old stars to that traced by young stars, but observations of the faint outer disk are technically challenging at any wavelength (see, e.g., de Jong 2008), particularly in the near-infrared. Fortunately, observations with *Spitzer* will provide a unique opportunity to explore the full extent of the stellar distribution with deep wide-field infrared imaging. Such observations are impossible to attempt from ground-based observatories due to the systematic and technical difficulties produced by generally variable sky levels and instruments with small areal coverage. Furthermore, comparable ground-based optical imaging is biased toward younger, star-forming disks and thus requires significantly longer integration times to achieve similar sensitivity to stellar mass; for instance, to image an old stellar population, R band imaging on a 4-m class telescope requires ~50 times the integration time to achieve a similar depth as our *Spitzer* 3.6 μm imaging. Figure 3 displays the ultraviolet, optical, and near-infrared surface brightness profiles and the stellar mass surface density profiles for the XUV galaxy NGC 5474. The dashed horizontal line indicates the expected sensitivity for our planned 1800 s/pix depth at 3.6 μm. Even if outer stellar disks could be detected in the optical, conversion from observed optical surface brightness to stellar mass density is highly dependent on the assumed stellar population age, initial mass function, and metallicity. Thus, observations with *Spitzer* is the only possible approach that will allow us to trace the stellar distribution to unprecedented levels at wavelengths that are insensitive to dust extinction and the galaxy's star formation.

1.2 Technical Plan

1.2.1 Sample Definition

Our sample of XUV galaxies originates from the comprehensive GALEX Ultraviolet Atlas of Nearby Galaxies (Gil de Paz et al. 2007). Galaxies with ultraviolet emission significantly beyond the de Vaucouleurs R_{25} radius were identified via ultraviolet surface brightness profiles (see Figures 1 and 2 for GALEX imaging of the sample). Gil de Paz and collaborators have undertaken a comprehensive ground-based campaign at Calar Alto to follow-up these XUV

targets with deep broadband and Hα imaging. Focusing on XUV galaxies with deep ancillary data allows for a detailed comparison of the spatially extended stellar populations spanning a wide range of ages. We have taken this subsample of the GALEX Atlas and further selected only moderate-size ($D_{25} < 5.5'$), high Galactic latitude galaxies ($|b| > 35$ degrees) within 20 Mpc that lack nearby companions, leaving us with a total of 12 XUV galaxies. Excluding galaxies at low Galactic latitudes minimizes contamination by foreground stars, and selecting only those with major optical diameters smaller than $5.5'$ avoids excessively long AORs. Adding a distance cut ensures reasonable spatial resolution (a $7''$ surface brightness profile bin width, for example, corresponds to 0.7 kpc at 20 Mpc). The balance between Type 1 and Type 2 XUV disks is similar to that found in the larger galaxy population found by Thilker et al. (2007).

To enable a fair interpretation of our 3.6 μm data on XUV galaxies, we have selected a control sample of non-XUV galaxies for which we also have access to deep GALEX ultraviolet and ground-based broadband and Hα imaging. The control sample is taken from the SINGS sample of nearby galaxies (Kennicutt et al. 2003; Dale et al. 2007), following the same selection criteria of $|b| > 35$ degrees and $D_{25} < 5.5'$. After further excluding the few SINGS galaxies lacking GALEX FUV and NUV imaging, the handful that already have deep IRAC imaging, and a couple targets that appear to be interacting with nearby neighbors, we are left with a control sample of six non-XUV SINGS galaxies where the ultraviolet emission is comparable in extent to that at optical wavelengths. The control sample includes a similar range of morphologies and optical sizes as those found in the primary science sample; issues such as foreground/background contamination and flat-fielding will be similar for the primary and control samples. As this project requires deep imaging with well-defined sky levels, we used SPOT to determine the typical infrared sky level for each target at both 3.6 and 4.5 μm. In all cases, the expected infrared sky levels are low, less than 0.1 MJy sr^{-1}. Taken as a whole, our survey of very deep 3.6 μm imaging will allow us to compare the extent and nature of the diffuse stellar distributions in galaxies exhibiting a wide variety of physical characteristics.

1.2.2 Observing Plan

We have analyzed the ultraviolet surface brightness profiles of our 17 XUV galaxies. The average ratio of R_{UV} to R_{25} for our XUV targets is 2.9; the typical XUV galaxy in our sample shows ultraviolet emission nearly three times as far out as the de Vaucouleurs optical radius. In terms of the 3.6 μm extent, Regan et al. (2006) find smoothly varying stellar surface brightnesses at 3.6 μm out to at least $1.5R_{25}$, and sometimes beyond $2R_{25}$, though the noise jumps dramatically for this radial regime at the SINGS imaging depth of just 240 s/pixel. Preliminary analysis of our far deeper (1800 s/pixel) Cycle 6 data on H I extended galaxies shows all 3.6 μm surface brightness profiles extend to at least $1.5R_{25}$ and some go as far as $2.5R_{25}$. In light of all these results, our proposed 3.6 μm observations are designed to map a field of view that corresponds to a factor of five beyond the de Vaucouleurs RC3 R_{25} radius. This will ensure enough coverage to adequately sample any extended stellar distributions while still allowing ample room for determining the sky value.

Astronomical Observing Requests (AORs) are constructed using the successful strategy utilized for our Cycle 6 program. Mosaics are built upon a grid of $100''$ spacings ($\sim$one-third the IRAC field of view). Two sets of maps will be obtained for each source to enable asteroid removal and data redundancy, and to build up the map sensitivity to the desired

level. Thus, at any given location within the map cores there will be a total of 18×100 s frames resulting in a net integration per sky position of 1800 s (along with a 1200 s $\sim 100''$-wide "inner periphery" and a 600 s, $\sim 100''$-wide "outer periphery"). The smallest maps will be 8x8 mosaics, ensuring at least $10'$ map cores at the deepest 1800 s effective integration. We will center the mosaics for 3.6 μm observations, but even our smallest maps have sufficient sky coverage that the field of view of the corresponding 4.5 μm mosaic will include the galaxy as well. We are submitting final AORs for this program.

Our sample is restricted to galaxies with low infrared sky levels (less than 0.1 MJy sr^{-1} at 3.6 μm), and thus we expect to achieve a 1σ noise level per pixel of 0.0018 MJy sr^{-1} at 3.6 μm (based on our Cycle 6 data and on SENS-PET predictions). Further, the simultaneous images at 4.5 μm will have a per pixel surface brightness sensitivity of 0.0027 MJy sr^{-1}; while the 4.5 μm mosaic will not be centered on the galaxy, it will provide both an independent observation of the extended stellar distribution and provide the potential to trace the faint stellar population to even larger radii (along the axis of observation).

These deep mosaics will allow us to trace the stellar distribution to unprecedented levels of a few $\times$ 0.01 $M_\odot$ pc^{-2}, at wavelengths that are relatively insensitive to dust and the galaxy's past star formation history. Figure 3 compares how sensitively our proposed 3.6 μm data will be able to detect stellar mass surface density in comparison to that using extant data at other wavelengths. Indeed, the 1800 s integration per position on the sky represents a much deeper effort than other surveys of nearby galaxies, e.g., SINGS ($N = 75; T = 240$ s; Kennicutt et al. 2003), LVL ($N = 258; T = 240$ s; Dale et al. 2009), S^{4}G ($N \sim 2300; T = 240$ s; Sheth et al. 2010), and the IRAC GTO project ($N = 100; T = 60$ or 150 s; Pahre et al. 2004). These surveys reach a 1σ sensitivity of a few to several kJy sr^{-1}, which is typically at the 5% level with respect to the mid-infrared surface brightness (Regan et al. 2006). With azimuthal averaging, our proposed observations will go below 1 kJy sr^{-1}, a necessity for obtaining high signal-to-noise in the faint outer disks beyond R_{25}.

1.2.3 Data Processing

The post-pipeline processing of the data should be straightforward, given our substantial experience with the SINGS, LVL, and our Cycle 6 programs. The multi-epoch, multiple-pointing observations for each galaxy will be combined into a single mosaic for each band using the MOPEX mosaicking software. Additional post-BCD processing will include distortion corrections, rotation of the individual frames (for multi-epoch observations), bias structure and bias drift corrections, image offset determinations via pointing refinements from the SSC pipeline, detector artifact removal, constant-level sky subtraction, and image resampling to 0.75$''$ pixels using drizzling techniques. The drizzling slightly improves the final PSF over the native one.

Based on experience with our Cycle 6 pilot program on HI extended galaxies, the two largest challenges to measuring stellar emission in the extreme outer disks are the presence of foreground stars/background galaxies and the stability of the sky levels within the large fields of view. As already explained above, we plan to limit the impact of the first issue by constraining our sample to $b > 35$ degrees. Furthermore, we have extensively explored how best to mask foreground stars and background galaxies. The optimal approach that we have converged upon relies on a two-pronged strategy. First, we identify foreground stars and background point sources using IRAF/DAOPhot. Second, we rely on SExtractor (Bertin & Arnouts 1996) to identify extended background galaxies. Empirical checks will be made on

these catalogs of foreground stars and background galaxies, via comparison with the Hα, ultraviolet, and broadband optical imaging. After these checks are made, foreground and background objects are masked as NaNs using an IDL script that utilizes the SExtractor ellipses for the extended targets and the SSC-provided IRAC 2D PSFs for the foreground stars and point sources.

To assess the stability of the sky levels within the large fields of view, we have analyzed the available maps from our Cycle 6 program that is being executed at the same imaging depth. Inspection of our mosaics, which span scales as large as $\sim$1 degree, shows sky variations less than 0.001 MJy sr^{-1}. Because our observing strategy has been and will be to map the entire field of view during each AOR (two per target), changes across the field due to variations in zodiacal light will be minimized. In short, we have adopted our Cycle 6 mapping strategy for this proposal, and that strategy has proven successful for a similar set of goals.

1.2.4 Data Analysis

An important parameter in deriving accurate surface brightness profiles is the sky value for each field. We will employ a curve of growth analysis to constrain sky levels in azimuthally averaged data. Once the sky level has been determined, azimuthal averages will allow us to probe surface brightness levels well below the single pixel detection limits (Figure 3). We will examine the derived surface brightness profiles in both 3.6 and 4.5 μm to look for evidence of disk truncation, as well as to examine the extent of the faint stellar distribution relative to the ultraviolet, optical, and Hα emission. Stellar masses will be computed using the 3.6 and 4.5 μm data, and star formation histories will be calculated based on the entire multi-wavelength dataset (e.g., Panter et al. 2007). The presence of 3.3 μm PAH emission in the IRAC1 band will likely be minimal due to the negligible dust present in outer disks (Gil de Paz et al. 2007; Dong et al. 2008), in addition to the fact that low metallicity depresses PAH emission (e.g., Engelbracht et al. 2008). The combination of these observations will yield the most extensive and deepest images of the faint stellar populations around nearby XUV galaxies.

1.2.5 Management Plan

As PI, Dale will coordinate the scientific efforts and management of the project, and serve as Technical Contact. Data processing, including mosaicking and curve of growth analysis, will be led by CoI Staudaher, who has extensive experience from our Cycle 6 projects described in § 3. All team members will participate in the analysis of the data. Gil de Paz and Thilker will provide expertise for the ultraviolet data, including post-pipeline-processed images and surface brightness profiles. Gil de Paz will also contribute analysis of his deep Hα and optical broadband imaging for the sample. van Zee and Barnes will lead on comparisons to the available H I data. Calzetti will provide expertise on stellar populations, including a comparison of multi-wavelength data of the outer disks to investigate the ages and characteristics of the stellar populations.
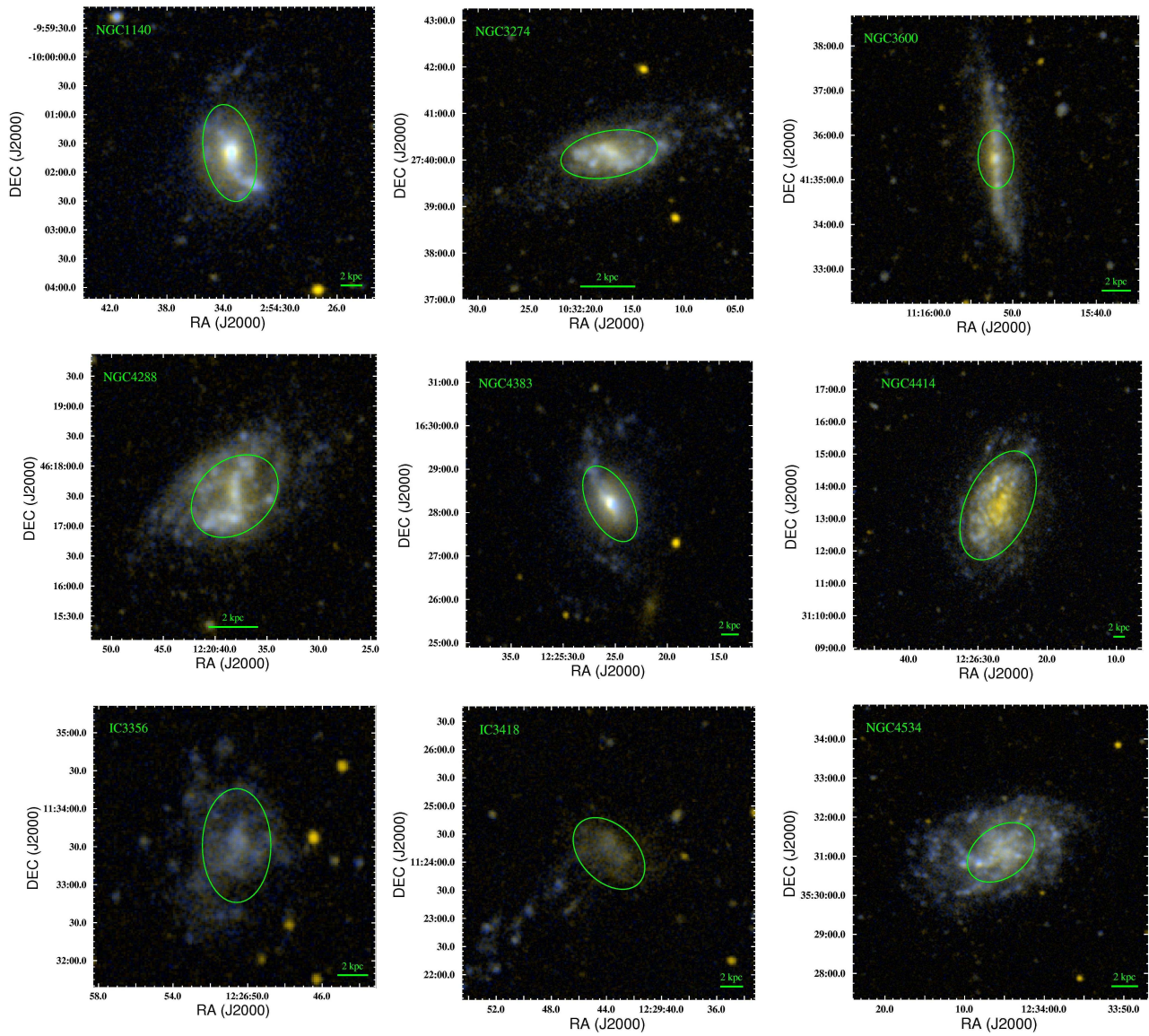
1.3 Figures, Tables & References

Figure 1: FUV-NUV false-color images for nine of the XUV galaxies in the sample. The ultraviolet emission extends well beyond the optical extent indicated by the $D_{25} \times d_{25}$ ellipses.
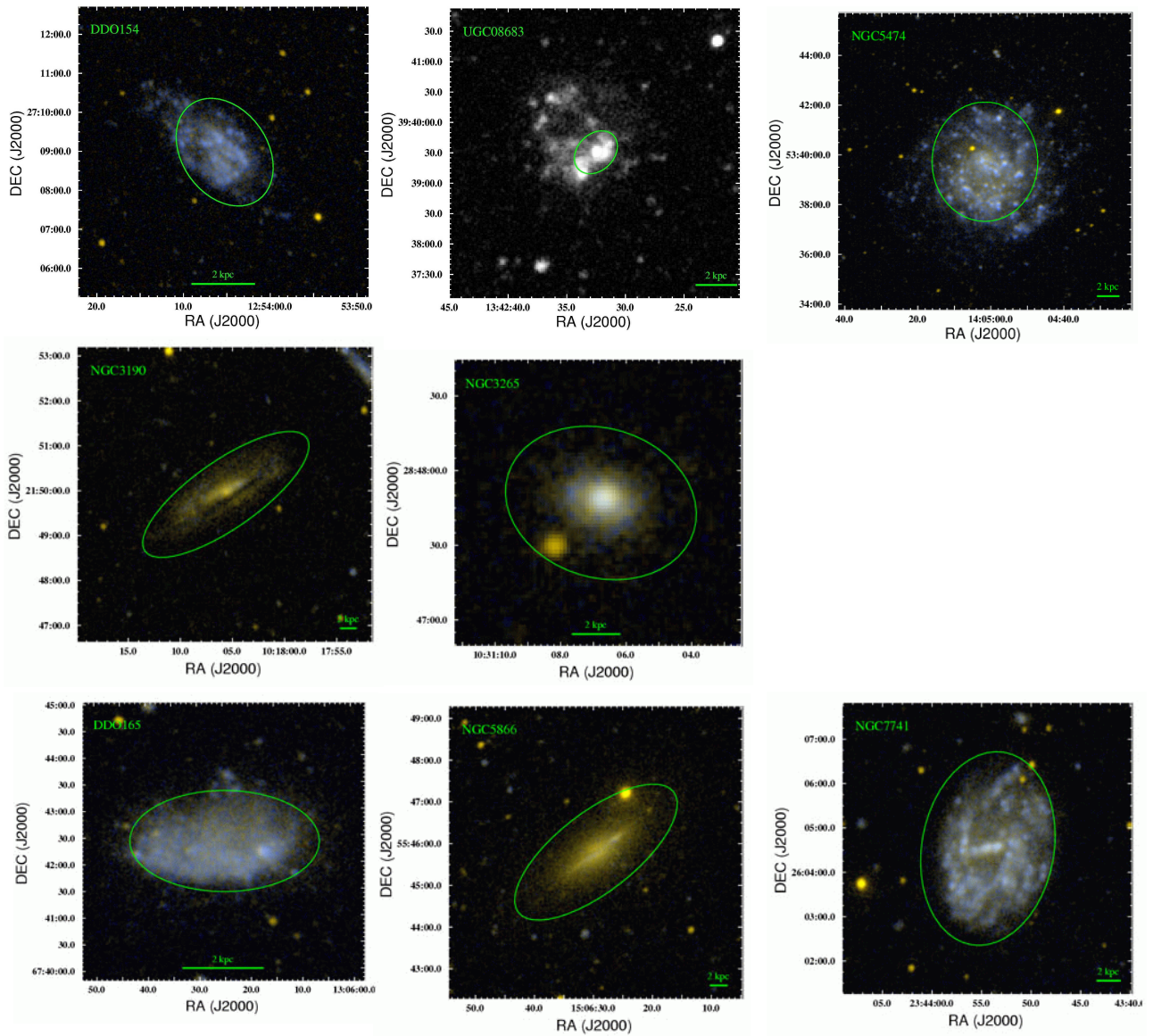
Figure 2: FUV-NUV false-color images for the remaining three XUV galaxies in the sample, followed by the six non-XUV galaxies in the control sample. The ellipses again are sized according to $D_{25} \times d_{25}$.
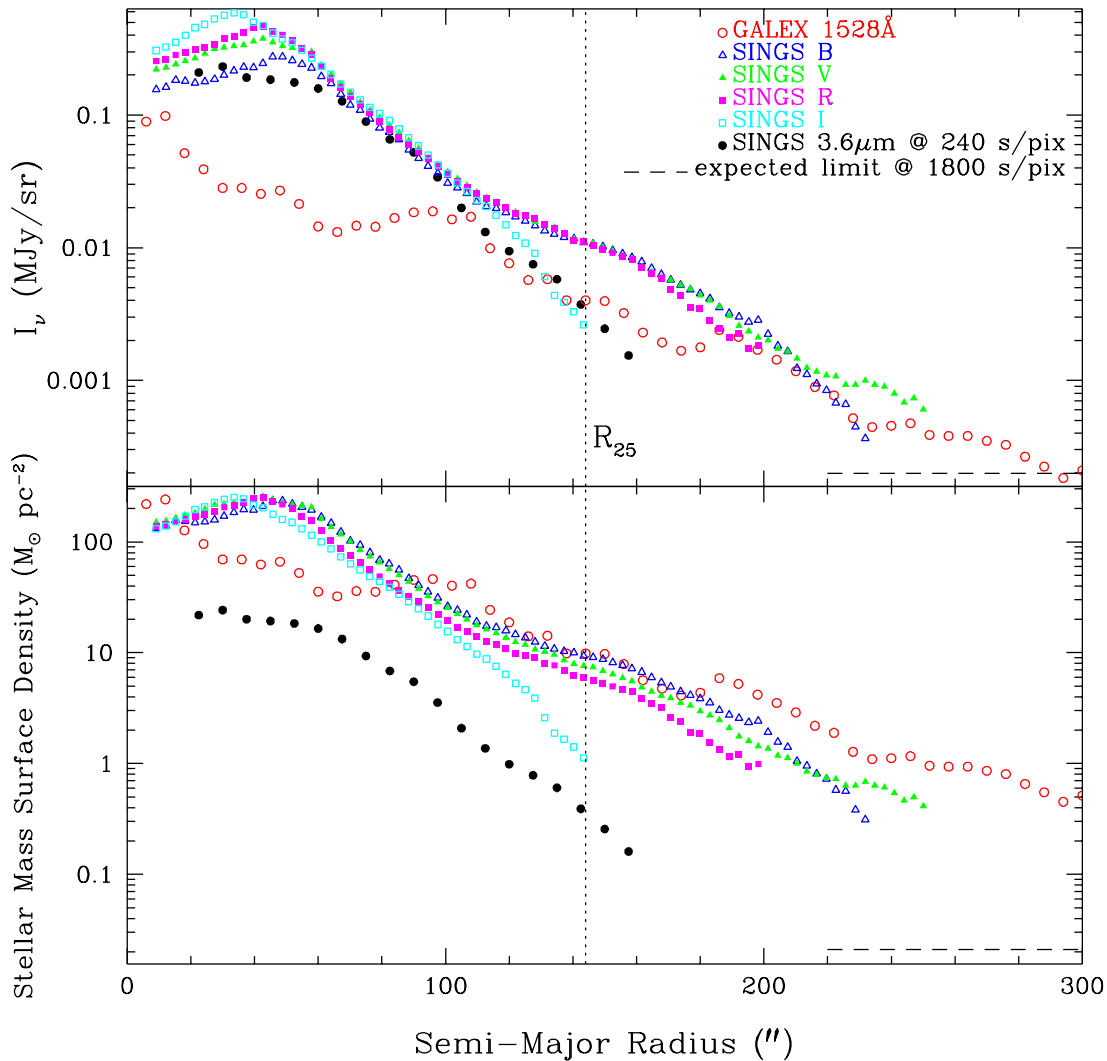
Figure 3: Top: The ultraviolet, optical, and near-infrared surface brightness profiles for XUV galaxy NGC 5474. The UV profile, shown with open red circles, extends far beyond R_{25}. The currently-available 3.6 μm surface brightness profile, shown with filled black circles, is at the relatively shallow depth provided by the SINGS survey (Dale et al. 2007). The predicted surface brightness limit for our survey is indicated by the dashed line. This expectation is based on SENS-PET predictions and is consistent with the preliminary analysis of our Cycle 6 program at the same imaging depth of 1800 s/pixel. Bottom: The stellar mass surface density profiles, assuming $M/L = 4M_{\odot}/L_{\odot}$ for a galaxy at 10 Mpc. The expected sensitivity to stellar mass with our proposed observations goes well below that available from extant data.

References

Abadi, M.G., Navarro, J.F., & Steinmetz, M. 2006, MNRAS, 365, 747

Alberts, S. et al. 2010, in preparation

Avila-Reese, V. & Firmani, C. 2000, RMxAA, 36, 23

Bertin, E. & Arnouts, S. 1996, A&AS, 117, 393

Bush, S.J., Hayward, C.C., Thilker, D., Hernquist, L., & Gurtina, B. 2010, ApJ, 713, 780

Christlein, D., Zaritsky, D., & Bland-Hawthorn, J. 2010, MNRAS, in press

Dale, D.A. et al. 2007, ApJ, 655, 863

Dale, D.A. et al. 2009, ApJ, 703, 517

de Jong, R.S. 2008, MNRAS, 388, 1521

Dong, H., Calzetti, D., Regan, M., Thilker, D., Bianchi, L., Meurer, G.R., & Walter, F. 2008, AJ, 136, 479

Engelbracht, C.W., Rieke, G.H., Gordon, K.D., Smith, J.-D.T., Werner, M.,W., Moustakas, J., Willmer, C.N.A., & Vanzi, L. 2008, ApJ, 678, 804

Gil de Paz, A. et al. 2007, ApJS, 173, 185

Goddard, Q.E., Kennicutt, R.C., & Ryan-Weber, E.V. 2010, MNRAS, in press

Gogarten, S.M., et al. 2009, ApJ, 691, 115

Governato, F., Mayer, L., Wadsley, J., Gardner, J.P., Willman, B., Hayashi, E., Quinn, T., Stadel, J., Lake, G. 2004, ApJ, 607, 688

Herbert-Fort, S. et al. 2009, ApJ, 700, 1977

Ibata, R., Chapman, S., Ferguson, A.M.N., Lewis, G., Irwin, M., & Tanvir, N. 2005, ApJ, 634, 287

Kennicutt, R.C. 1998, ARAA, 36, 189

Kennicutt, R.C. et al. 2003, PASP, 115, 928

Kennicutt, R.C. Lee, J.C., Funes, S.J.Jose G., Sakai, S., & Akiyama, S. 2008, ApJS, 178, 247

Kroupa, P. & Weidner, C. 2003, ApJ, 598, 1076

Krumholz, M.R., McKee, C.F., & Tumlinson, J. 2009, ApJ, 699, 850

Lee, J.C. et al. 2009, ApJ, 706, 599

Leroy, A.K., Walter, F., Brinks, E., Bigiel, F., de Blok, W.J.G., Madore, B., Thornley, M.D. 2008, AJ, 136, 2782

Martin, C.L. & Kennicutt, R.C. 2001, ApJ, 555, 301

Meurer, G.R. et al. 2009, ApJ, 695, 765

Pahre, M.A., Ashby, M.L.N., Fazio, G.G., & Willner, S.P. 2005, ApJS, 154, 235

Panter, B., Jimenez, R., Heavens, A.F., & Charlot, S. 2007, MNRAS, 378, 1550

Pflamm-Altenburg, J., Weidner, C., & Kroupa, P. 2007, ApJ, 671, 1550

Pflamm-Altenburg, J., Weidner, C., & Kroupa, P. 2009, MNRAS, 395, 394

Pohlen, M. & Trujillo, I. 2006, 454, 759

Regan, M. et al. 2006, ApJ, 652, 1112

Robertson, B., Yoshida, N., Springel, V., & Hernquist, L. 2004, ApJ, 606, 32

Rogstad, D.H., Lockart, I.A, & Wright, M.C.H. 1974, ApJ, 193, 309

Roškar, R., Debattista, V.P., Stinson, G.S., Quinn, T.R., Kaufmann, T., Wadsley, J. 2008 ApJL, 684, L79

Schmidt, M. 1959, ApJ, 129, 243

Thilker, D.A. et al. 2005, ApJL, 619, L79

Thilker, D.A. et al. 2007, ApJS, 173, 538

van den Bergh, S. 1980, PASP, 92, 122

Weidner, C. & Kroupa, P. 2005, ApJ, 625, 754

Weidner, C. & Kroupa, P. 2007, MNRAS, 365, 1333

Zaritsky, D. & Christlein, D. 2007, AJ, 134, 135

2 Brief Team Resume

Daniel A. Dale (Wyoming) is an expert on studies of star formation from low- to intermediate-redshift, as well as on the infrared spectra and panchromatic broadband spectral energy distributions of normal galaxies. He has extensive experience with *Spitzer* observations and data processing, as a CoI on SINGS, as a CoI on the Cycle 4 Local Volume Legacy Project (LVL), and as a CoI on the two Cycle 6 projects described in the next section.
Kate L. Barnes (Indiana) is an astronomy graduate student. Her Ph.D. dissertation examines star formation rate indicators in the outer edges of spiral galaxies. She is PI on a Cycle 6 study of the extended disk in M 83.
Daniela Calzetti (UMass) is an expert on multi-wavelength observations of star formation activity in nearby galaxies. She is a member of the SINGS, LVL, among other related *Spitzer* programs.
Armando Gil de Paz (UC Madrid) is an expert on the multi-wavelength emission from normal galaxies and blue compact dwarf galaxies. He is a member of the SINGS and LVL legacy teams, is a leading expert on GALEX observations of galaxies, including those with extended ultraviolet emission.
Shawn M. Staudaher (Wyoming) is a post-baccalaureate research assistant who will begin his graduate studies this fall at Wyoming. He has led the IRAC data processing and mosaic construction for the two Cycle 6 programs described in the following section.
David Thilker (Johns Hopkins) is an expert on the multi-wavelength properties of nearby galaxies. His discovery of extended ultraviolet emission in M 83 has led to intense efforts to understand star formation in galaxy peripheries.
Liese van Zee (Indiana) is an expert on galaxy formation and evolution with an emphasis on investigating the links between star formation, elemental enrichment, and gas distribution and kinematics in star-forming galaxies. She has extensive experience working with multi-wavelength data sets (UV, optical, IR, and radio). She is PI of a Cycle 6 program on Hɪ extended disks described in the following section, and is CoI on LVL.

Selected Related Publications
The Calibration of Mid-Infrared Star Formation Rate Indicators
     Calzetti et al. 2007, ApJ, 666, 870
An Ultraviolet-to-Radio Broadband Spectral Atlas of Nearby Galaxies
     Dale et al. 2007, ApJ, 655, 863
The *Spitzer* Local Volume Legacy: Survey Description and Infrared Photometry
     Dale et al. 2009, ApJ, 703, 517
The GALEX Ultraviolet Atlas of Nearby Galaxies
     Gil de Paz et al. 2007, ApJS, 173, 185
A Search for Extended Ultraviolet Disk (XUV-Disk) Galaxies in the Local Universe
     Thilker et al. 2007, ApJS, 173, 538
Spectroscopy of Outlying Hɪɪ Regions in Spiral Galaxies: Abundances and Radial Gradients
     van Zee et al. 1998, AJ, 116, 2805

3　Summary of Existing Programs

Liese van Zee is the PI of 60094, a 69.7-hour Cycle 6 Warm Mission program to probe the older stellar population in the outskirts of galaxies with extended H<small>I</small> disks. Four of the nine galaxies have been observed so far. For these four galaxies we have post-pipeline processed the data, optimized the creation of their image mosaics, developed routines for masking foreground stars and background galaxies, extracted surface brightness profiles, and compared the radial extent of the older population to the H<small>I</small> radius.

Kate Barnes is the PI of 60116, a 30.2-hour Cycle 6 Warm Mission program to probe the extended older stellar population in M 83. The first half of the imaging dataset was taken on 05 April 2010, and the second half on 11 April 2010. We have not yet received the pipeline data.

Daniel Dale is Technical Contact for the above two programs. Dale is leading the data processing efforts on these two programs.

Daniela Calzetti is the PI of 20289 and 30753, Cycle 2 and 3 programs to probe the star formation and dust content in the outer parts of nearby galaxies. Results from the first program are published (Dong et al. 2008) and the data for the second project are under analysis.

4   Observation Summary Table

Galaxy	Position (J2000)	$D_{25} \times d_{25}$ (arcmin)	D_{UV}/ D_{25}	# grid points	AOR (hrs)	$f(K_{\mathrm{s}})$ (Jy)	Type
NGC1140	025433.6−100140	1.7×0.9	3.0	8x 8	4.1	0.042	XUV 2
NGC3274	103217.3+274008	2.1×1.0	3.0	8x 8	4.1	0.036	XUV 2
NGC3600	111552.0+413527	1.3×0.8	3.6	8x 8	4.1	0.055	XUV 1
NGC4288	122038.1+461730	1.6×1.2	2.8	8x 8	4.1	0.032	XUV 1
NGC4383	122525.5+162812	1.9×1.0	3.5	8x 8	4.1	0.106	XUV 1
NGC4414	122627.1+311325	3.6×2.0	1.9	13x13	10.6	1.110	XUV 1
IC3356	122650.5+113332	1.5×0.9	2.4	8x 8	4.1		XUV 1
IC3418	122943.8+112409	1.5×1.0	2.7	8x 8	4.1		XUV 1
NGC4534	123405.4+353106	1.9×1.3	3.2	8x 8	4.1	0.150	XUV 2
DDO154	125405.3+270859	3.0×2.2	2.3	11x11	7.6	0.012	XUV 2
UGC08683	134232.5+393930	0.8×0.6	5.6	8x 8	4.1		XUV 1.5
NGC5474	140312.5+542056	4.8×4.3	2.2	16x16	16.0	0.114	XUV 1.5
NGC3190	101805.6+214956	4.4×1.5	1.0	15x15	14.1	0.741	non-XUV
NGC3265	103106.7+284748	1.3×1.0	1.2	8x 8	4.1	0.048	non-XUV
NGC3773	113813.0+120644	1.2×1.0	1.1	8x 8	4.1	0.035	non-XUV
DDO165	130624.8+674225	3.5×1.9	1.4	13x13	10.6	0.037	non-XUV
NGC5866	150629.5+554504	4.7×1.9	1.1	16x16	16.0	1.263	non-XUV
NGC7741	234354.4+260432	4.4×3.0	1.2	15x15	14.1	0.094	non-XUV

There are 133.9 hrs total requested for this observing program.

5   Modification of the Proprietary Period

No modification to the proprietary period is requested for this program.

6   Summary of Duplicate Observations

There are no duplicate observations. Observations by the SINGS (P00159), LVL (P40204), and S^{4}G (P61060-8) for NGC 3077, NGC 3185, NGC 3274, NGC 3600, NGC4288, IC 3356, NGC 4534, DDO 154, UGC08331, NGC 5474, NGC 3190, NGC 3265, NGC 3773, DDO 165, NGC 5866, and NGC 7793 do not have the depth (2×4×30 s/pix=240 s/pix) and field of view to constitute our observations as duplications. A few programs have observed a handful of other galaxies, and again our duplications are deeper and more extended to not be considered duplications: NGC 1140 (P00059), NGC 4383 (P30945), NGC 4414 (P00069), NGC 4477 (P03649; P40936), NGC 7741 (P00069).

7   Summary of Scheduling Constraints/ToOs

There are no scheduling constraints or ToOs in this program.